PROCEEDINGS, 41st Workshop on Geothermal Reservoir Engineering
Stanford University, Stanford, California, February 22-24, 2016
SGP-TR-209

Least-Squares Reverse-Time Migration with Compressive Sensing for Sparse Seismic Data

Youzuo Lin[1], Lianjie Huang[1], John Queen[2], Joseph Moore[3] and Ernest Majer[4]

1. Los Alamos National Laboratory, Geophysics Group, Los Alamos, NM 87545; 2. Hi-Q Geophysical Inc., Ponca City, OK 74601; 3. University of Utah, Salt Lake City, UT 84108; 4. Lawrence Berkeley National Laboratory, Berkeley, CA 94720

ylin@lanl.gov, ljh@lanl.gov, john.h.queen@gmail.com, jmoore@egi.utah.edu, elmajer@lbl.gov

Keywords: Least-squares reverse-time migration, vertical seismic profile, compressive sensing, sparse seismic data

ABSTRACT

Least-squares reverse-time migration yields better images than the conventional reverse time migration. However, images of least-squares reverse-time migration may still contain significant artifacts for sparse seismic data when source/receiver intervals are too large. We develop a novel least-squares reverse-time migration method with compressive sensing to improve migration imaging with sparse seismic data. Our method incorporates an L_p-norm-based compressive sensing term in the objective function of least-squares reverse-time migration. We employ an alternating-minimization algorithm to solve the optimization problem of our new least-squares reverse-time migration method. We validate our new method using synthetic vertical seismic profiling (VSP) data from a geophysical model built using geologic features and well log data at the Raft River geothermal field. We apply our method to synthetic VSP data for a sparse source array and compare the results with those obtained with a dense source array. Our new migration method produces an image using a sparse source array with image quality similar to that obtained using a dense source array.

1. INTRODUCTION

Reverse-time migration (RTM) solves the full-wave equation in heterogeneous media to obtain high-resolution migration images (Baysal et al. 1983; Yoon et al. 2003; Etgen et al. 2009). Least-squares reverse-time migration (LSRTM) can improve migration images when data are sparse (Tang 2009; Dai and Schuster 2013; Tan and Huang 2014). However, when data are too sparse, LSRTM may produce images with significant artifacts. Several different approaches were developed to improve LSRTM imaging (Wang and Sacchi 2005; Sacchi et al. 2006; Aoki and Schuster 2009; Xue et al. 2014; Tan and Huang 2014). Wang and Sacchi (2005) and Sacchi et al. (2006) adapted quadratic and non-quadratic regularization (Cauchy norm) in LSRTM to improve the resolution while suppressing the spatial artifacts. Aoki and Schuster (2009) developed an LSRTM method with a deblurring filter. They used the deblurring filter either as a part of the regularization term or as a preconditioner of the inversion. Xue et al. (2014) incorporated a structure-enhancing filter in the regularization term. Tan and Huang (2014) developed an improved LSRTM method using updated source fields and a wavefield-separation imaging condition. LSRTM with the L_1 norm based regularization term (Cauchy norm, or total-variation norm) can preserve interfaces better than that with the quadratic norms. However, L_1 norm-based LSRTM also suffers from the non-differentiality at the origin.

We develop a new least-squares reverse-time migration method with an L_p-norm based compressive sensing scheme (LSRTM-CS) to improve image quality and reduce image artifacts when data are extremely sparse. We employ the sparsity in the gradient domain because of its success in other applications such as medical imaging and image analysis (Sidky et al. 2013). To promote the sparsity of the inversion, L_1-norm related minimization is usually used. Chartrand (2012) shows that an L_p norm minimization yields more accurate results than the conventional compressive sensing technique using L_1-norm minimization. This also changes the conventional compressive sensing from a convex optimization problem to a nonconvex optimization. To solve the nonconvex minimization problem, we use an alternating direction method of minimization (ADMM) (Bauschke et al. 2006), which leads to a computationally very efficient algorithm. We validate the capability of our new LSRTM-CS using synthetic VSP data for a geophysical model built using geologic features found at the Raft River geothermal field (Ayling and Moore 2013). Our numerical example demonstrates that our new least-squares reverse-time migration method preserves the accuracy of the imaging results using only a fraction of seismic data needed for conventional least-squares reverse-time migration.

2. LEAST-SQUARES REVERSE-TIME MIGRATION

Reverse-time migration (RTM) solves the full-wave equation in heterogeneous media for forward source and backward receiver wave propagation. The relationship between seismic data p and reflectivity model m is governed by

$$p = Lm, \tag{1}$$

where L is the forward wave propagation operator. RTM imaging is to solve

$$m = L^T p, \tag{2}$$

where adjoint operator L^T approximates the inverse of L. LSTRM solves the minimization problem

$$E(m) = min_m\{\|d - Lm\|_2^2\}, \tag{3}$$

where d is recorded seismic data. Solving Eq. (3) yields a migration image m that minimizes the mean square difference between recorded and synthetic seismic data.

3. LEAST-SQUARES REVERSE-TIME MIGRATION WITH COMPRESSIVE SENSING (LSRTM-CS)

We employ the compressive sensing technique (Sidky et al. 2013; Chartrand 2012) in least-squares reverse-time migration, and the cost function becomes

$$E(m) = min_m\{\|d - Lm\|_2^2 + \lambda\|\nabla m\|_p^p\}, \tag{4}$$

where $0 \le p \le 1$, λ is a positive regularization parameter, and the compressive sensing term, $\|\nabla m\|_p^p$, for a 2D model is defined as the L_p-norm given by

$$\|\nabla m\|_p^p = \sum_{i,j}(|(\nabla_x m)_{i,j} + (\nabla_z m)_{i,j}|)^p. \tag{5}$$

We select $p = 1/2$ according to Chartrand (2012). Similar to Chartrand (2012), we employ an alternating direction method of minimization to solve the Eq. (4).

4. NUMERICAL RESULTS

We use synthetic VSP data for a geophysical model shown in Fig. 1a to validate the capability of our new least-squares reverse-time migration method with compressive sensing to handle sparse seismic data. This geophysical model is constructed using geologic features found at the Raft River geothermal field (Ayling and Moore 2013). It contains two major fault zones that have been identified on the west side of the valley: the Bridge fault zone and the Horse Wells fault zone. The model also contains a vertical narrow zone in the middle near the bottom of the model. For the dense source array, a total of 160 sources are evenly distributed with a spatial interval of 15 m at the top surface of the model. Simulating a VSP, 162 receivers are placed along a borehole as shown in Fig. 1a. The receivers are located between 0.5 km and 1.8 km in depth. A Ricker wavelet with a center frequency of 40 Hz is used as the source function. We smooth the original velocity model in Fig. 1a by averaging the slowness within one wavelength, resulting in the model in Fig. 1b. We use this smoothed model as the starting model for our least-squares reverse-time migration.

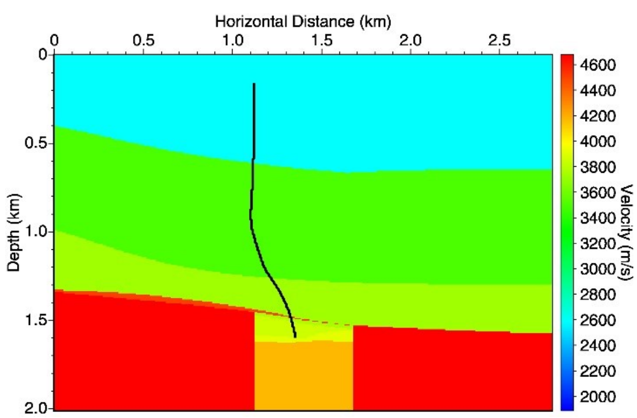

(a)

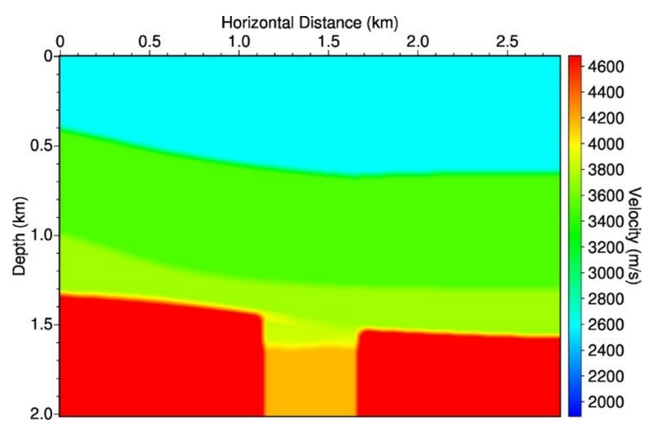

(b)

Figure 1: Velocity models used for LSRTM: (a) true velocity model from Raft River geothermal field for generating synthetic VSP data; (b) smoothed velocity model used as the starting model for LSRTM. The vertically curved line in (a) is the borehole location for VSP receivers.

We first compare the performance of our LSRTM-CS migration for a sparse source array with that of LSRTM for dense source array. Figure 2a shows the result of LSRTM using all seismic data, and Fig. 2b displays the result of our LSRTM-CS using only one tenth of the original data (i.e. one tenth of the total number of seismic sources). The LSRTM-CS yields an imaging result similar to that obtained using LSRTM with a dense source array.

The result of LSRTM can be sensitive to the starting velocity models. To further understand the robustness of the LSRTM-CS , we test the method using two initial models shown in Fig. 3. Figure 3a is the initial model obtained by smoothing the true model within two wavelengths and Fig. 3b is the initial model obtained by smoothing the true model within three wavelengths. Figure 4 shows the imaging results using the initial model in Fig. 3a. Figure 5 displays the imaging results using the initial model in Fig. 3b. Our method using the sparse array in Fig. 4b yields a similar result to that obtained using LSRTM with the dense source array depicted in Fig. 4a. Similarly, the imaging results shown in Fig. 5 are comparable to one another using both dense and sparse source arrays. Therefore, our new LSRTM-CS method is robust to the initial model.

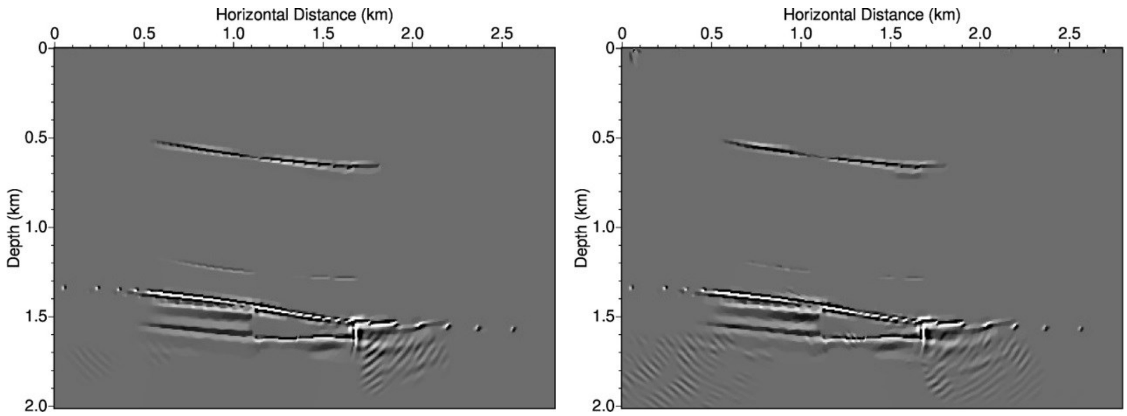

(a) (b)

Figure 2: Migration images of synthetic VSP seismic data obtained using: (a) the conventional LSRTM with a dense source array; and (b) our LSRTM-CS method with a sparse source array (i.e. one tenth of the total number of sources in the dense source array).

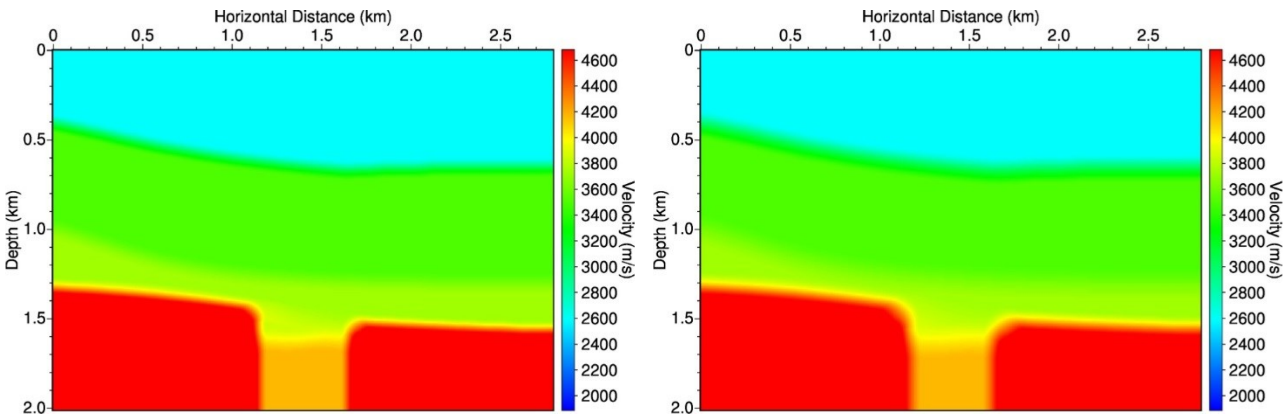

(a) (b)

Figure 3: Velocity models smoothed within: (a) two wavelengths; and (b) three wavelengths used as the starting models for LSRTM.

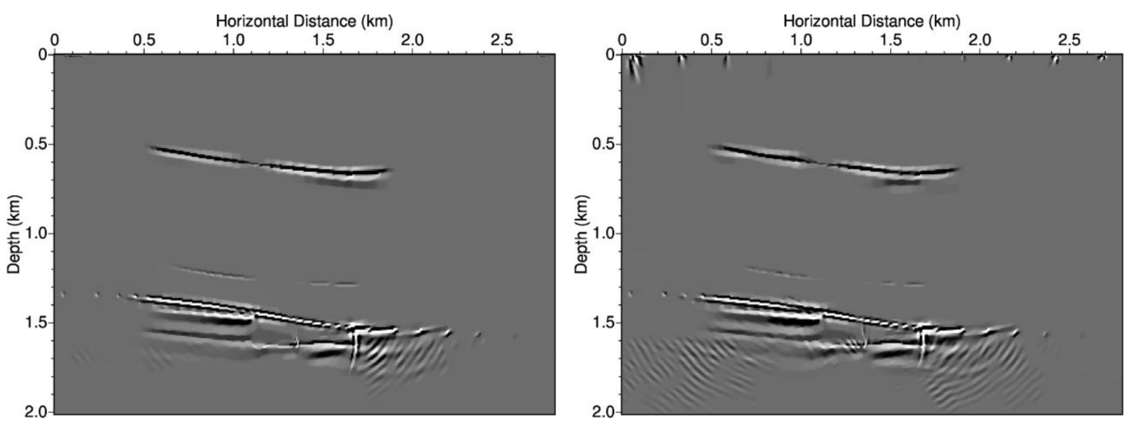

(a) (b)

Figure 4: Migration images of synthetic VSP seismic data obtained using: (a) the conventional LSRTM with a dense source array; and (b) our LSRTM-CS method with a sparse source array (i.e. one tenth of the total number of sources in the dense source array). The starting model used is the one in Fig. 3a.

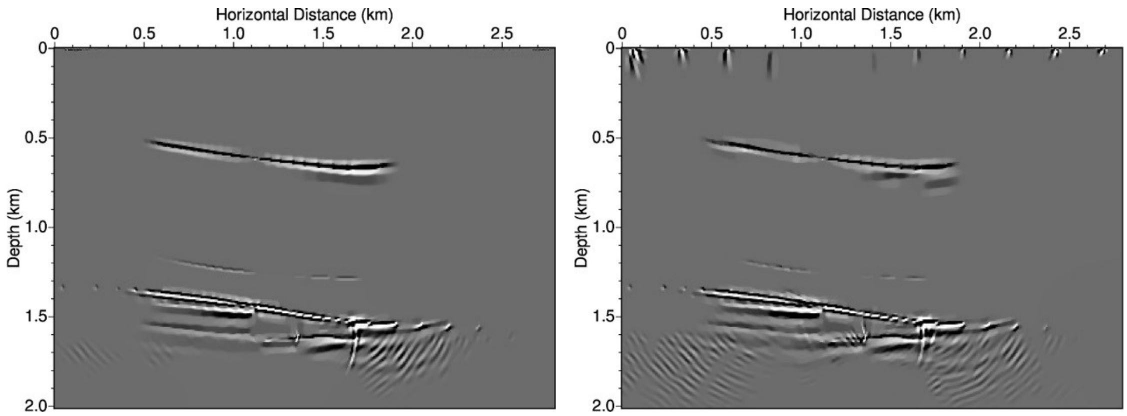

(a) (b)

Figure 5: Migration images of synthetic VSP seismic data obtained using: (a) the conventional LSRTM with a dense source array; and (b) our LSRTM-CS method with a sparse source array (i.e. one tenth of the total number of sources in the dense source array). The starting model used is the one in Fig. 3b.

5. CONCLUSIONS

We have developed a novel least-squares reverse-time migration method with an L_p-norm-based compressive sensing technique for imaging with sparse seismic data. The method employs an L_p-norm in the penalty term. We have validated the capability of our new least-squares reverse-time migration method using only a fraction of seismic data acquired with a dense seismic source array. Our least-squares reverse-time migration results of synthetic VSP data for the Raft River geothermal field demonstrate that our new method can preserve the accuracy of least-squares reverse-time migration for sparse seismic data.

6. ACKNOWLEDGEMENTS

This work was supported by the Geothermal Technologies Office of the U.S. Department of Energy through contract DE-AC52-06NA25396 to Los Alamos National Laboratory. The computation was performed on super-computers provided by the Institutional Computing Program of Los Alamos National Laboratory.

REFERENCES

Aoki, N., and Schuster, G.: Fast least-squares migration with a deblurring filter, *Geophysics*, **74**, (2009), WCA83–WCA93.

Ayling, B., and Moore, J.: Fluid geochemistry at the Raft River geothermal field, Idaho, USA: New data and hydrogeological implications, *IEEE Trans. Signal Process*., **47**, (2013) 116–126.

Bauschke, H., Combettes, P. and Noll, D.: Joint minimization with alternating Bregman proximity operators, *Pacific Journal of Optimization*, **2**, (2006), 401–424.

Baysal, E., Kosloff, D. and Sherwood, J.: Reverse time migration, *Geophysics*, **48**, (1983), 1514–1524.

Chartrand, R.: Nonconvex splitting for regularized low-rank + sparse decomposition, *IEEE Trans. Signal Process.*, **60**, (2012), 5810–5819.

Dai, W., and Schuster, G.: Plane-wave least-squares reverse-time migration, *Geophysics*, **78**, (2013), S165–S177.

Etgen, J., Gray, S. and Zhang, Y.: An overview of depth imaging in exploration geophysics, *Geophysics*, **74**, (2009), WCA5–WCA17.

Goldstein, T. and Osher, S.: The split Bregman method for l1 regularized problems, *SIAM Journal on Imaging Sciences*, **2**, (2009), 323–343.

Huang, Y., NG, M. and Wen, Y.: A fast total variation minimization method for image restoration, *SIAM Journal on Multiscale Modeling and Simulation*, **7**, (2008), 774–795.

Lin, Y. and Huang, L.: Acoustic- and elastic-waveform inversion using a modified total-variation regularization scheme, *Geophysical Journal International*, **200**, (2015), 489–502.

Nocedal, J. and Wright, S.: Numerical optimization, (2000), Springer.

Rudin, L., Osher, S. and Fatemi, E.: Nonlinear total variation based noise removal algorithms, *Physica D.*, **60**, (1992), 259–268.

Sacchi, M., Wang, J. and Kuehl, H.: Regularized migration/inversion: new generation of imaging algorithms, *CSEG Recorder*, Special Edition, (2006), 54–59.

Sidky, E. Y., Chartrand, R., Jorgensen, J. S. and Pan, X.: Nonconvex optimization for improved exploitation of gradient sparsity in CT image reconstruction, 12th International Meeting on Fully Three-Dimensional Image Reconstruction in Radiology and Nuclear Medicine, (2013), 189–192.

Tan, S. and Huang, L.: Least-squares reverse-time migration with a wavefield-separation imaging condition and updated source wavefields, *Geophysics*, **79**, (2014), S195–S205.

Tang, Y.: Target-oriented wave-equation least-squares migration/inversion with phase-encoded Hessian, *Geophysics*, **74**, (2009), WCA95–WCA107.

Wang, J. and Sacchi, M. Sparse regularization for least-squares AVP migration, CSEG National Convention, Expanded Abstracts, (2005), 117–120.

Wang, Y., Yang, J., Yin, W. and Zhang, Y.: A new alternating minimization algorithm for total variation image reconstruction, *SIAM Journal on Imaging Sciences*, **1**, (2008), 248–272.

Xue, Z., Chen, Y., Fomel, S. and Sun, J.: Imaging incomplete data and simultaneous-source data using least squares reverse-time migration with shaping regularization, 84th Annual International Meeting, SEG, Expanded Abstracts, (2014), 3991–3996.

Yoon, K., Shin, C., Suh, S., Lines, L. and Hong, S.: 3D reverse-time migration using the acoustic wave equation: An experience with the SEG/EAGE data set, *The Leading Edge*, **22**, (2003), 38–41.

Zhang, Z., Lin, Y. and Huang, L.: Full-waveform inversion in the time domain with an energy-weighted gradient, 81th Annual International Meeting, SEG, Expanded Abstracts, (2011), 2772–2776.